



**Credit: 2 PDH**

**Course Title:**

***Condensation Heat Transfer on  
Geometrically Enhanced Horizontal Tube***

**Approved for Credit in All 50 States**

Visit [epdhone.com](http://epdhone.com) for state specific information including Ohio's required timing feature.

**3 Easy Steps to Complete the Course:**

1. Read the Course PDF
2. Purchase the Course Online & Take the Final Exam
3. Print Your Certificate

---

# Condensation Heat Transfer on Geometrically Enhanced Horizontal Tube: A Review

---

Hafiz Muhammad Ali

Additional information is available at the end of the chapter

<http://dx.doi.org/10.5772/65896>

---

## Abstract

In this chapter, an attempt has been made to present the recent state of knowledge of free-convection condensation heat transfer on geometrically enhanced tubes. This survey is divided into three sections. The first section concentrates on research on condensate flooding or retention. The second and the third sections cover the experimental and the theoretical work on geometrically enhanced tubes, respectively.

**Keywords:** phase change, heat transfer, condensation, horizontal tube, geometrically enhanced tubes, enhancement, integral fins, pin fins, model

---

## 1. Introduction

The phenomenon of condensation heat transfer has been researched for over a century now. In the beginning, the primary focus to increase heat transfer was kept limited to the increase in surface area. Later, it was revealed that surface-tension forces play a vital role in thinning the condensate layer which in turn increases heat transfer. The mechanism of condensation heat transfer on two-dimensional integral-fin tubes is now well understood. Researchers have successfully identified the optimum geometries, fin shapes, dimensions and materials for integral-fin tubes for a wide range of condensing fluids. A number of theoretical models, for instance Briggs and Rose [1], Ali and Briggs [2], have successfully combined the effect of surface tension and gravity to explain condensation heat transfer on integral-fin and pin-fin tubes. However, relatively fewer investigations have been carried out for condensation on three-dimensionally enhanced tubes.

This chapter presents a state-of-the-art review of condensation heat transfer on single-horizontal geometrically enhanced tubes. The problem of condensate retention on geometrically

---

enhanced tubes has been reviewed in detail followed by the experimental and theoretical investigations of condensation heat transfer on integral-finned and pin-finned tubes.

## 2. Free-convection condensation on horizontal smooth tubes

The first investigator to propose a theoretical model of condensation heat transfer on vertical plates and horizontal tubes was Nusselt [3]. By considering laminar flow and constant properties for the condensate film, uniform temperature on the vapour side (no temperature gradient in the vapour), and neglecting inertia, convection in the condensate film (i.e. heat transfer across the condensate film occurs only by conduction) and shear stress at the condensate surface, the following results were obtained:

For a vertical plate:

$$Nu_P = 0.943 \left[ \frac{\rho(\rho - \rho_v)gh_{fg}L^3}{\mu k \Delta T} \right]^{1/4} \quad (1)$$

For a horizontal tube:

$$Nu_T = 0.728 \left[ \frac{\rho(\rho - \rho_v)gh_{fg}d^3}{\mu k \Delta T} \right]^{1/4} \quad (2)$$

Many theoretical investigations have since been carried out including factors neglected by Nusselt [3] such as convection in condensate, shear stress and inertia (for instance, Sparrow and Gregg [4], Koh et al. [5] and Chen [6, 7]). The inclusion of these parameters made little practical difference to the results of Nusselt [3]. Rose [8] reports a comprehensive literature review of theoretical studies of laminar-film condensation on smooth tubes.

## 3. Free-convection condensation on horizontal-enhanced tubes

### 3.1. Condensate retention or flooding

It is well understood that heat-transfer rate is strongly influenced by the available area. For that reason, a long time ago smooth tubes were replaced by horizontal integral-fin tubes. No doubt, the addition of the fins provides an increase in area that ultimately leads to an enhancement in heat transfer, but a significant amount of condensate is retained on the tube due to capillary forces. This phenomenon of trapped liquid between fins is known as ‘condensate retention or flooding’ and is illustrated in **Figure 1**. This condensate offers a great resistance to heat transfer. A flooding angle,  $\phi_f$ , has been defined to indicate the point from the top of the tube, where the condensate flooding completely fills the inter-fin spacing up to the tip of the fin. This problem of condensate retention was first experimentally investigated by Katz et al. [9].

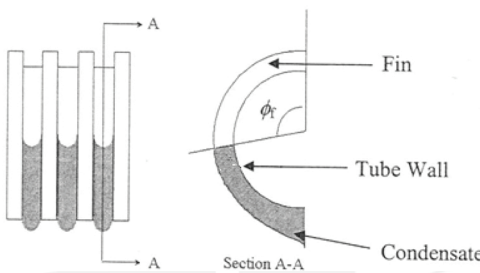


Figure 1. Condensate flooding on a horizontal integral-fin tube showing retention angle  $\Phi_f$ .

Rudy and Webb [10, 11] reported experimental investigations of condensate retention on three integral-fin tubes and a spine-fin tube with fin densities in a range of 748–1378 fins per meter using n-pentane, R-11 and water under static (without condensation) and dynamic (with condensation) conditions. For all the fluids, they found an increase in condensate retention with increasing fin density and surface-tension-to-density ratio. They also found no significant differences in condensate retention under static and dynamic conditions.

Honda et al. [12] presented a comprehensive experimental and theoretical analysis of condensate flooding using R-113 and methanol on three horizontal integral-fin tubes and a saw-toothed tube with and without 'drainage strips'. A significant decrease in condensate retention was reported when the same tubes were used with drainage strips. One of the integral-fin tubes was tested under both static and dynamic conditions and no significant change in condensate retention was observed which was in line with the findings of Rudy and Webb [10].

Honda et al. [12] made the following assumptions for their theoretical analysis of the static meniscus between trapezoidal fins:

1. The meniscus is just in contact with the fin tip.
2. The radius of curvature of the condensate interface is much smaller in the longitudinal direction than in the circumferential direction.
3. The fin height ( $h$ ) and the fin-tip spacing ( $b$ ) are sufficiently smaller than the fin-tip radius ( $R_o$ ).
4. The radius of curvature at the tube bottom is infinite in the longitudinal direction.

Using the above assumptions, the following expression was produced for retention angle,  $\Phi_f$ , measured from the top of the tube:

$$\Phi_f = \cos^{-1} \left[ \left( \frac{2\sigma \cos \theta}{\rho g b R_o} \right) - 1 \right] \quad (3)$$

where

$$h > (s/2) \cos \theta \quad (4)$$

Honda et al. [12] compared their own experimental data, experimental data of Katz et al. [9] and experimental data of Rudy and Webb [10] using Eq. (3). Good agreement was found between experiment and theory. Later, Rudy and Webb [11] and Owen et al. [13] obtained the same Eq. (3) of condensate-retention angle for integral-fin tubes.

Yau et al. [14] reported experimental data for condensate-retention angle using fluids steam, ethylene glycol and R-113. Thirteen tubes with rectangular integral fins were tested with a fin height of 1mm, a thickness of 0.5mm and a variable-fin spacing. For tubes with  $h > s/2$ , the measured retention angles showed good agreement using Eq. (3) as shown in **Figure 2**. Two tubes with fin spacing of 1.5 and 2mm were also tested using copper-drainage strips; a significant increase in the retention angle was noted. The following empirical expression was determined for the retention angle of tubes using drainage strips:

$$\phi_f = \cos^{-1} \left( \frac{0.83\sigma}{\rho g b R_o} - 1 \right) \quad (5)$$

**Figure 2** also shows a good agreement of experimental data using Eq. (5). A provisional equation for trapezoidal integral-fin tubes using drainage strips was also suggested as

$$\phi_f = \cos^{-1} \left( \frac{0.83\sigma \cos \theta}{\rho g b R_o} - 1 \right) \quad (6)$$

Masuda and Rose [15] comprehensively analyzed the configuration of the liquid film retained by surface-tension forces on horizontal low integral-fin tubes ( $h \ll R_o$ ). This study revealed that

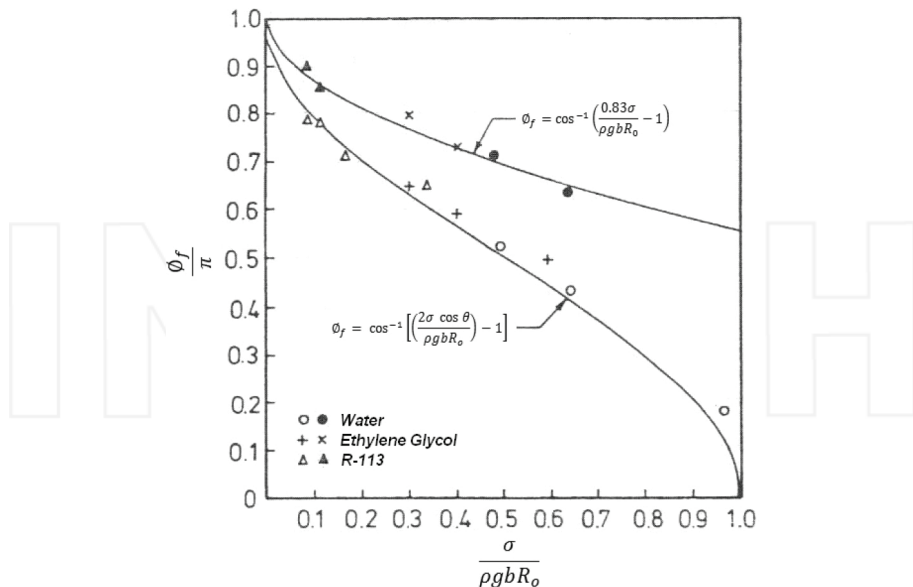
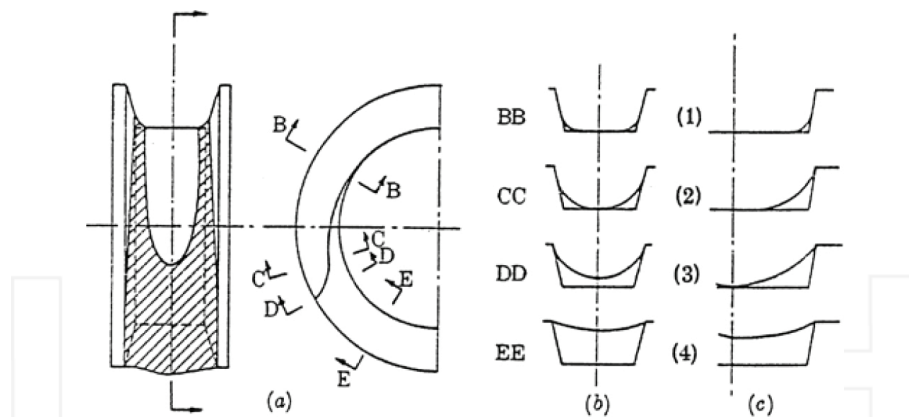


Figure 2. Liquid retention results with and without drainage strips (after Yau et al. [14]).



**Figure 3.** Configuration of retained liquid or condensate around a horizontal integral-fin tube. (a) Condensate retention on integral-fin tube. (b) Configuration of liquid around the narrow-spaced integral-fin tube. (c) Configuration of liquid around the wide-spaced integral-fin tube (after Masuda and Rose [15]).

the liquid is not only retained on the lower part of the tube (below the retention angle) but also on the upper part of the tube surface in the form of ‘wedges’ between fin flanks and tube surface in the inter-fin space. This phenomenon is illustrated in **Figure 3**. **Figure 3b** and **c** describes the configuration of liquid around the tube for narrow-spaced ( $h > (s/2) \cos \theta$ ) and wide-spaced ( $h < (s/2) \cos \theta$ ) integral-fin tubes, respectively. Four ‘flooding’ conditions were identified for trapezoidal fins and the positions around the tube at which these occur were determined:

For narrow-spaced fins ( $h > (s/2) \cos \theta$ ), where the inter-fin space is just filled by the meniscus but the fin flanks are not wholly wetted (**Figure 3b.2**). Retention angle,  $\phi_f$ , for this case is given as

$$\cos \phi_f = \left( \frac{2\sigma}{\rho g s R_r} \right) \left[ \frac{\cos \theta}{1 + \sin \theta} \right] - \left( \frac{R_o}{R_r} \right) \quad (7)$$

For narrow-spaced fins ( $h > (s/2) \cos \theta$ ), where the whole flank is just wetted (contact angle at the fin tip is zero) and for which the liquid film at the centre of the inter-fin space has finite thickness (**Figure 3b.3**). This is the condition for which Honda et al. [12] derived flooding angle Eq. (3). Retention angle,  $\phi_f$ , for this case is given as

$$\cos \phi_f = \left( \frac{2\sigma}{\rho g b R_o} \right) \cos \theta - 1 \quad (8)$$

For wide-spaced fins ( $h < (s/2) \cos \theta$ ), where the fin flanks are wholly wetted (contact angle at the fin tip is zero) before the inter-fin space is flooded (**Figure 3c.2**). Retention angle,  $\phi_f$ , for this case is given as

$$\cos \phi_f = \left( \frac{\sigma}{\rho g h R_r} \right) (1 - \sin \theta) - \left( \frac{R_o}{R_r} \right) \quad (9)$$

For wide-spaced fins ( $h < (s/2) \cos \theta$ ), where the whole of the inter-fin space is just flooded and the contact angle at the fin tip is no longer zero (Figure 3c.3). Retention angle,  $\phi_f$ , for this case is given as

$$\cos \phi_f = \left( \frac{8\sigma h}{\rho g(b^2 + 4h^2)R_o} \right)^{-1} \quad (10)$$

Masuda and Rose [15] also defined an ‘active area enhancement ratio’ for low-rectangular integral-fin tubes (when  $h > s/2$ ) as ‘The unblanked area of a finned tube (i.e. area of fin tips plus area of unblanked part of fin flanks plus area of unblanked part of inter-fin tube surface) divided by the area of a smooth tube with radius equal to the fin root radius’. The following equation was derived for active area-enhancement ratio,  $\xi$ ,

$$\xi = \frac{R_r b \phi_f (1 - f_s) + (R_o^2 - R_r^2) \phi_f (1 - f_f) + \pi R_o t}{\pi R_r (b + t)} \quad (11)$$

where  $f_s$  and  $f_f$  are the blanked proportions of the inter-fin space and fin flanks for the unflooded part of rectangular-finned tube, respectively, and are given by the following expressions:

$$f_s = \left( \frac{2\sigma}{\rho g b R_r} \right) \left\{ \frac{\tan(\phi_f/2)}{\phi_f} \right\} \quad (12)$$

and

$$f_f = \left( \frac{\sigma}{\rho g h R_r} \right) \left\{ \frac{\tan(\phi_f/2)}{\phi_f} \right\} \quad (13)$$

Rose [16] extended the work and proposed expressions for  $f_s$  and  $f_f$  for trapezoidal-finned tubes as

$$f_s = \left\{ \frac{1 - \tan(\theta/2)}{1 + \tan(\theta/2)} \right\} \left( \frac{2\sigma}{\rho g b R_r} \right) \left\{ \frac{\tan(\phi_f/2)}{\phi_f} \right\} \quad (14)$$

and

$$f_f = \left\{ \frac{1 - \tan(\theta/2)}{1 + \tan(\theta/2)} \right\} \left( \frac{\sigma}{\rho g h R_r} \right) \left\{ \frac{\tan(\phi_f/2)}{\phi_f} \right\} \quad (15)$$

It was suggested by Masuda and Rose [15] that manufacturing integral-fin tubes with filleted fin roots would replace the retained wedges of condensate with high-conductivity metal, and

hence increase the active area-enhancement ratio resulting in more heat transfer. Wen et al. [17] experimentally investigated the effect of fillet fin roots on heat-transfer enhancement using steam, ethylene glycol and R-113 as condensing fluids on four integral-fin tubes. A significant enhancement was found for tubes with filleted roots over tubes without filleted roots.

Briggs [18] obtained static liquid-retention measurements on 12 three-dimensional pin-fin tubes and three integral-fin tubes. R-113, ethylene glycol and water were used as test fluids. Static retention measurements were obtained by using two methods: first by taking photographs and second by counting pins. A comparison of both methods of measuring retention angles is shown in **Figure 4**; it can be seen for water and ethylene glycol, and both methods give results within 15%, but for R-113, pin-counting method gives higher-retention angles compared to the photographic method. Finally, retention angles for water and ethylene glycol were taken as the average of both the methods, but for R-113, pin-counting method was used as it was deemed more accurate than photographic method. Liquid retention on three-dimensional pin-fin tubes was found to be lower than the equivalent integral-fin tubes (i.e. with the same longitudinal- and radial-fin dimensions). The controlling parameters appeared to be longitudinal and circumferential pin spacing. A tube with 1-mm circumferential spacing was found to be optimum for flooding angle. Pin height and longitudinal and circumferential pin thickness had little influence on retention.

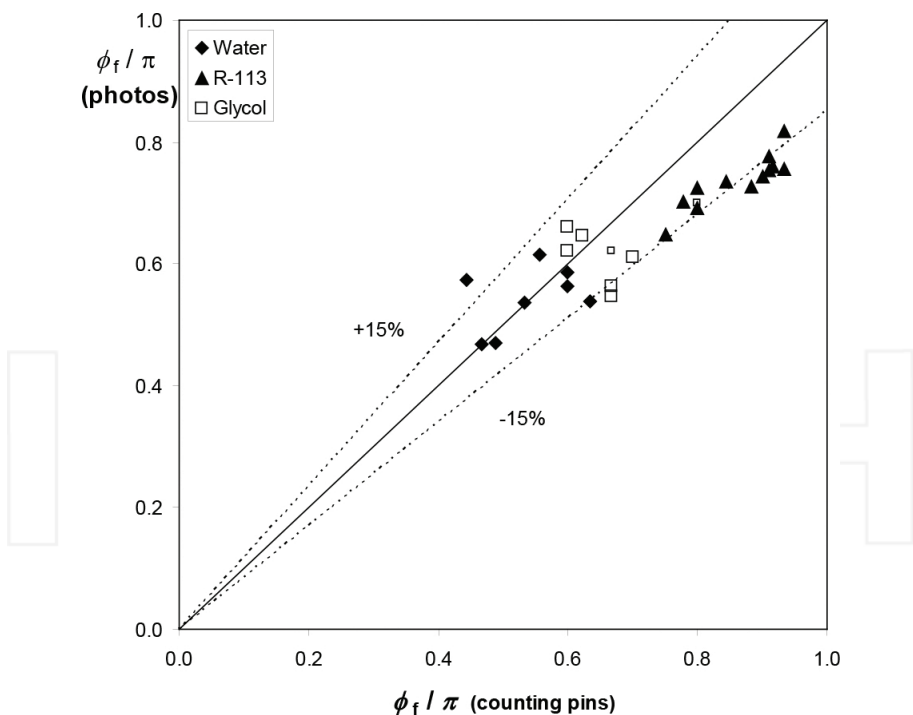


Figure 4. Comparison of pin-counting method with photographic method by Briggs [18].

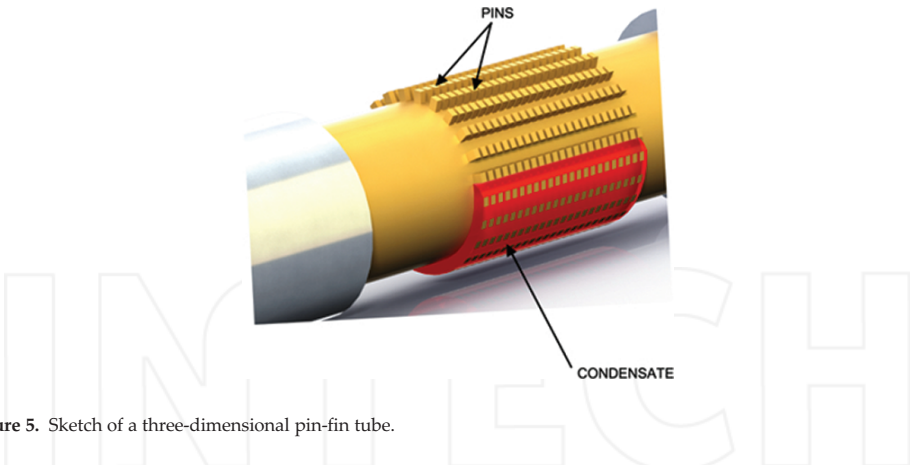


Figure 5. Sketch of a three-dimensional pin-fin tube.

Comprehensive experimental data for condensate retention (for free convection) were reported on 15 pin-fin tubes (**Figure 5**) by Ali and Briggs [19]. Static method to create condensate was adopted to carry out experimentation. Pin-counting and photographic methods were used to analyse condensate and a comparison of both methods was found to be within  $\pm 5\%$ . All pin-fin tubes were found to be less flooded than the equivalent integral-fin tubes. A semi-empirical model was also reported for condensate-retention angle on pin-fin tubes as follows:

$$\phi_f = \cos^{-1} \left[ \left( 1 - \left( 0.4919 - 1.306 \left( \frac{\sigma}{\rho R^2 g} \right) \frac{s_c}{t_c} \right) \left( \frac{2\sigma}{\rho g s R_o} \right) - 1 \right) \right] \text{ for } s < 2h \quad (16)$$

Ali and co-workers [20–22] have reported in detail studies on condensate retention as a function of vapour velocity on horizontal integral-fin and pin-fin tubes. Recently, Ali et al. [23] reported the effect of condensate flow rate on retention angle for horizontal integral-fin tubes.

### 3.2. Experimental studies into condensation heat transfer on enhanced tubes

**Table 1** summarizes the key facts and figures of experimental investigations carried out on enhanced tubes which are described in detail in the following sections.

#### 3.2.1. Tubes with two-dimensional fins

Honda et al. [12] presented heat-transfer measurements for the condensation of R-113 and methanol on three integral-fin tubes and a three-dimensional saw-toothed tube. The vapour-side, heat-transfer coefficient was found by direct measurements (12–16 thermocouples were placed in each tube wall). The saw-toothed tube gave the best heat-transfer enhancements (defined as heat-transfer coefficient for saw-toothed tube based on fin-tip diameter divided by the heat-transfer coefficient for a smooth tube at the same vapour-side, temperature difference) for both fluids which was 9.0 and 6.1 for R-113 and methanol, respectively.

Investigation	Number of tubes tested	Type of tube	Heat-transfer coefficient calculation method	Fluids tested	Maximum reported heat-transfer enhancement ratio
Honda et al. [12]	4	3 trapezoidal integral fin saw-toothed	Direct measurements	R-113/Methanol	9.06.1
Yau et al. [24]	13	Rectangular integral fin	Predetermined coolant-side correlation	Steam	3.6
Masuda and Rose [25]	14	Rectangular integral fin	Predetermined coolant-side correlation	R-113	7.3
Masuda and Rose [26]	14	Rectangular integral fin	Predetermined coolant-side correlation	Ethylene glycol	4.4
Wanniarchchi et al. [27, 28]	24	Rectangular integral fin	Predetermined coolant-side correlation	Steam	5.2
Marto et al. [30]	24	Rectangular integral fin	Modified Wilson plot	R-113	7.0
Sukathme et al. [34]	12	9 trapezoidal integral fins/3 Pin fins	Direct measurements	R-11	10.3 (integral fin)/12.3 (pin fin)
Briggs et al. [31]	6	Rectangular integral fin	Direct measurements	R-113/Ethylene glycol/steam	6.84.83.0
Briggs et al. [35]	17 (commercial tubes)	7 two-dimensional/10 three-dimensional	Predetermined coolant-side correlation	R-113	8.2
Kumar et al. [37]	2	1 integral fin/1 pin fin	Modified Wilson plot and direct measurements	Steam	2.5 (integral fin)/3.6 (pin fin)
Kumar et al. [39]	8	2 integral fins/2 pin fins/4 partial integral fins	Direct measurements	Steam/R-134a	2.96.5
Briggs [41]	6	Pin-fin tubes	Predetermined coolant-side correlation	R-113/steam	9.92.9
Park et al. [33]	4	Integral fin	Direct measurements	R-123	5.8
Baisier and Briggs [42]	5	Pin fin	Predetermined coolant-side correlation	Steam	4.1

Table 1. Summary of experimental literature review.

Yau et al. [24] reported an experimental study of dependence of heat transfer on fin spacing for the condensation of steam on horizontal integral-fin tubes. Thirteen tubes with rectangular fins having a thickness of 0.5 mm and a height of 1.6 mm were tested by systematically varying fin spacing from 0.5 to 20 mm. All tubes were having a fin-root diameter of 12.7 mm. A plain tube with an outer diameter equal to the fin-root diameter was also tested for comparison. All tests were performed at near-atmospheric pressure with vapour flowing vertically downward with velocities between 0.5 and 1.1 m/s. The vapour-side, heat-transfer coefficients were found by subtracting the predetermined coolant side and wall resistance from the overall thermal resistance. The observed heat-transfer enhancement for integral-fin tubes significantly exceeded the increase in active area. The maximum vapour-side, heat-transfer enhancement was found to be around 3.6 for the tube with a fin spacing of 1.5 mm. Integral-fin tubes with a spacing of 0.5 and 1.0 mm were found to be almost completely flooded by condensate.

Yau et al. [14] also used solid drainage strips with two integral-fin tubes of fin spacing of 1.5 and 2.0 mm and found that for steam the drainage strip significantly reduced the condensate flooding. The drainage strips were made of copper having a thickness of 0.5 mm and a height of 8 mm. The tubes with strips provided about 25–30% additional heat-transfer enhancement compared to the same integral-fin tubes without strips.

Masuda and Rose [25, 26] reported experimental data for the condensation of R-113 and ethylene glycol on integral-fin tubes. The effect of fin spacing was investigated on the same set of tubes as used by Yau et al. [14, 24] with the inclusion of a new integral-fin tube with a fin spacing of 0.25 mm. Predetermined coolant-side correlation and a modified Wilson plot method were used to evaluate the vapour-side, heat-transfer coefficients. For both condensing fluids vapour-side, heat-transfer enhancement was found to be about two times higher than the corresponding active area. Tubes with a spacing of 0.5 and 1.0 mm showed best heat-transfer enhancement of 7.3 for R-113 and 4.4 for ethylene glycol, respectively.

Masuda and Rose [15] summarized the above experimental investigations by plotting the dependence of vapour-side, heat-transfer enhancement against fin spacing. For steam, ethylene glycol and R-113, tubes with a fin spacing of 1.5, 1 and 0.5 mm, respectively, gave the best heat-transfer enhancement. They also plotted a graph of active-area enhancement against fin spacing. For steam, ethylene glycol and R-113, integral-fin tubes with a fin spacing of 1.5, 1 and 0.5 mm gave the best active-area enhancement, respectively. Thus, heat-transfer enhancement is a maximum for fin spacing that maximize the active area.

Wanniarachchi et al. [27, 28] reported vapour-side, heat-transfer measurements for the condensation of steam at atmospheric and low (11.3 kPa) pressure on 24 horizontal rectangular cross-section integral-fin tubes made of copper. Fin spacing (0.5, 1.0, 1.5, 2.0, 4.0 mm), fin thickness (0.5, 0.75, 1.0 and 1.5 mm) and fin height (0.5, 1.0, 1.5 and 2.0 mm) were changed systematically to find the best geometry for heat transfer. Vapour-side, heat-transfer coefficients were obtained using a predetermined coolant-side correlation and also by a modified Wilson plot method. Enhancement ratio was found to be strongly dependent on fin spacing and an optimum value was reported between 1.5 and 2.0 mm for all tubes. Fin thickness showed a weak effect on enhancement ratio with an optimum range between 0.75 and 1.0 mm.

Enhancement ratio was found to increase with increasing fin height but at a lower rate than the area increase.

Marto et al. [29] presented an experimental study to identify the optimum fin shape to maximize heat transfer. Four integral-fin tubes with rectangular, triangular, trapezoidal and parabolic fin shapes were tested using steam as the condensing fluid. All tubes had a same fin height and fin-root spacing and thickness. Tests were carried out at near-atmospheric and below-atmospheric pressures. A tube with a roughly parabolic fin shape outperformed the tubes with rectangular, triangular and trapezoidal fin shapes at both pressures.

Marto et al. [30] reported experimental data condensing R-113 on 24 integral-fin tubes and a commercially available tube. Fin spacing was varied systematically in a range of 0.25–4 mm for different sets of fin thicknesses. All tests were performed at a little above atmospheric pressure with a downward-flowing vapour velocity of 0.4 m/s. Vapour-side, heat-transfer coefficients were obtained using the modified Wilson plot method with a measured uncertainty in the range of  $\pm 7\%$ . The tube with a fin spacing of 0.25 mm and a thickness of 0.5 mm gave the best heat-transfer enhancement of 7 for a corresponding area enhancement of 3.9. For all tubes tested, heat-transfer enhancements were found to be considerably higher than the corresponding increase in active areas. The best fin spacing was obtained to be in between 0.2 and 0.5 mm, depending upon the corresponding fin thickness and height. Heat-transfer coefficient was also found to increase with increase in fin height, but the rate of increase in coefficient of heat transfer was found to decrease with the increase in height.

Briggs et al. [31] reported experimental data for the condensation of steam, ethylene glycol and R-113 on two sets of integral-fin tubes. The smaller tubes had a fin-root diameter of 12.7 mm, fin thickness 0.5 mm and fin height 1.6 mm, whereas the larger tubes had a fin-root diameter of 19.1 mm and fin thickness and height of 1.0 mm. For both types, three fin spacings of 0.5, 1.0 and 1.5 mm were tested. The outside tube-wall temperature was measured directly by four embedded thermocouples. For all the smaller tubes, tests were conducted at a little above atmospheric pressure. For larger tubes, tests were performed at a little above atmospheric pressure for steam and R-113 and also at lower pressures of 3 and 14 kPa for ethylene glycol and steam, respectively. For both larger and smaller diameters, the best-performing integral-fin tubes were found with fin spacings of 1.5, 1.0 and 0.5 mm for steam, ethylene glycol and R-113, respectively. They compared their own experimental data with the indirectly obtained experimental data of earlier investigators [24, 27, 28, 30] and a satisfactory agreement was found.

Briggs et al. [32] reported systematic experimental data for the condensation of steam and R-113 on rectangular integral-fin tubes made of copper, brass and bronze, with fin spacing and fin-root diameter of 1.0 and 12.7 mm, respectively; fin heights and thicknesses varied in the range of 0.5–1.6 mm and 0.25–0.75 mm, respectively. For R-113, the heat-transfer enhancement was weakly dependent on fin thermal conductivity but more strongly dependent on fin height and thickness, whereas for steam, the effect of thermal conductivity on heat-transfer enhancement was much stronger for larger fin heights, but the effect of fin height and thickness was relatively small.

Park et al. [33] obtained experimental data for R-123 condensing on four integral-fin tubes used in building chillers with varying fin density in a range of 10 fins per inch to 36 fins per inch. A plain tube with the same outside diameter was also tested to compare the results. The vapour-side, heat-transfer coefficients were found directly with embedded thermocouples in the tube wall. The tube with a fin density of 28 fins per inch was found to be optimum with a vapour-side, heat-transfer enhancement of 5.8.

### *3.2.2. Tubes with three-dimensional fins*

Sukathme et al. [34] obtained experimental data for the condensation of R-11 on nine horizontal integral-fin tubes and three special pin-fin tubes made of copper and reported the effect of fin height, fin density and fin-tip angle on vapour-side, heat-transfer coefficients. All tubes were made with trapezoidal fin shapes. Vapour-side, heat-transfer coefficients were found from directly measured tube-wall temperatures, obtained by placing 15 thermocouples at 5 positions along the tube and at top, bottom and mid-plane around the tube. Fin-tip angle showed a small effect on the vapour-side, heat transfer, whereas fin density and fin height showed considerable effects on the vapour-side, heat-transfer coefficient. The best-performing integral-fin tube with a fin density of 1417 fins per meter, a fin height of 1.22mm and a fin-tip angle of 10° gave a vapour-side, heat-transfer of 10.3 with a corresponding active-area enhancement of 7. Further, 80 longitudinal trapezoidal grooves were machined in the best-performing integral-fin tube with three different heights of 0.7, 0.9 and 1.22mm. The authors reported a large increase in vapour-side, heat-transfer enhancements with increasing value of height. The pin-fin tube with a longitudinal groove height of 1.22mm gave a heat-transfer enhancement of 12.3 which was about 20% more than the equivalent best-performing integral-fin tube. The authors suggested that this increase in heat-transfer enhancement could be due to the increase in the flooding angle of the pin-fin tube which was about 20% more than the corresponding integral-fin tube.

Briggs et al. [35] reported experimental data for the condensation of R-113 on 17 commercially available copper integral-fin tubes. These consisted of seven two-dimensional tubes (Gewa N and K, trapezoidal cross section) and ten three-dimensional tubes (one thermoexcel and nine petal shaped). It was found that the best two-dimensional tube (K-50) and best three-dimensional tube (P8) gave similar vapour-side, heat-transfer enhancement of 8.2.

Cheng et al. [36] obtained condensing data for R-22 on six commercially available tubes. Two tubes had low integral fin, whereas four were three-dimensionally enhanced. One set of tubes consisting of an integral-fin tube, an externally enhanced tube and an externally plus internally enhanced tube has a fin density of 26 fins per inch, fin pitch of 0.97mm and a height of 1.3mm, whereas the other set of tubes consisting of one integral-fin tube, one externally enhanced tube and one externally plus internally enhanced tube has a fin density of 40 fins per inch, fin pitch of 0.61mm and a fin height of 1.42mm. Experiments were carried out at three different pressures of 1.3, 1.5 and 1.6MPa. A Wilson plot method was used to obtain vapour-side, heat-transfer coefficients. The three-dimensional externally plus internally enhanced tubes showed the highest heat-transfer coefficients compared to rest of the tubes. The heat-transfer coefficients were found to decrease with increasing value of pressure. It was also found that vapour-

side, heat-transfer coefficients decreased more sharply for three-dimensionally enhanced tubes as a function of increasing temperature difference compared to integral-fin tubes.

Kumar et al. [37] reported experimental data for the condensation of steam on a plain tube with an outside diameter of 22mm and an integral-fin tube (with an outside diameter of 25 mm, fin height of 1.1mm, fin thickness of 1.1mm and fin spacing of 1.5mm). A three-dimensional pin-fin tube was also tested with similar radial and longitudinal dimensions as of integral-fin tube but with 40 axial grooves around the circumference producing a circumferential pin spacing of 0.9mm. The condensing-side heat-transfer coefficients were found using a modified Wilson plot method and also by direct measurement of wall temperatures; good agreement was found between the two methods. Vapour-side, heat-transfer enhancements of 2.5 and 3.6 were found for the integral-fin tube and pin-fin tube, respectively. The superior performance of the pin-fin tube was thought to be primarily due to the thinning of the condensate film by the surface-tension pull in two directions in the unflooded area as also proposed by Sukhatme et al. [34] condensing R-11 and also due to the improved condensate drainage at the bottom of the tube. Authors reported the improved condensate drainage at the bottom part of the pin-fin tube compared to the condensate drainage for the integral-fin tube.

Jung et al. [38] reported vapour-side, heat-transfer enhancements for an integral-fin tube with fin density of 26 fins per inch and a three-dimensional turbo-C tube with a fin density of 42 fins per inch condensing two low-pressure (R-11 and R-123) and two medium-pressure (R-12 and R-134a) refrigerants. A plain tube was also tested for comparison. Vapour-side, heat-transfer coefficients were obtained directly by measuring the tube-wall temperature with embedded thermocouples. For low-pressure refrigerants, heat-transfer coefficients for R-123 of about 8–19% lower than those of R-11 were found for all tubes tested. For medium-pressure refrigerants, heat-transfer coefficients for R-134a were about 0–32% higher than those for R-12. The vapour-side, heat-transfer enhancements for turbo-C and integral-fin tubes based upon the plain tube area were roughly reported up to 8.0 and 5.5, respectively.

Kumar et al. [39, 40] presented experimental data for the condensation of steam and R-134a. Five tubes consisting of one plain, one integral-fin, one pin-fin and two partial integral-fin tubes (i.e. one with pin fins on the upper half and one with pin fins on the lower half) were tested for each fluid. For steam, all enhanced tubes had rectangular fins and a fin density of 390 fins per meter, whereas for R-134a, all enhanced tubes had trapezoidal fins and a fin density of 1560 fins per meter. Pin-fin tubes were made by machining longitudinal grooves into integral-fin tubes. Pin-fin tubes gave the best vapour-side, heat-transfer enhancements of 2.9 for steam (30% more than equivalent integral-fin tube tested) and 6.5 for R-134a (24% more than equivalent integral-fin tube tested). Pin fins were reported to be more effective at lower half of the tube than the upper half of the tube, that is, for steam, a heat-transfer enhancement of 2.4 (with pin fin on the upper half) and 2.7 (with pin fins on the lower half), whereas for R-134a, a heat-transfer enhancement of 5.7 (with pin fins on the upper half) and 6.3 (with pin fins on the lower half) was reported. Tubes with pin fins on the lower half outperformed the equivalent integral-fin tubes by up to 20% for steam and 11% for R-134a. For R-134a, pin fins on the upper half of the tube did not contribute in the heat-transfer enhancement but showed 5% improvement for steam compared to integral-fin tube.

Briggs [41] reported experimental data for the condensation of R-113 and steam on six three-dimensional pin-fin tubes. These tubes were made by machining rectangular longitudinal grooves into integral-fin tubes. A plain tube with the same outside diameter as the pin-fin tube-root diameter was also tested for comparison purposes. The vapour-side, heat-transfer coefficient was obtained by subtracting the coolant and wall resistances from the measured overall resistance. For R-113, the best-performing tube had circumferential pin thickness and spacing of 0.5mm, pin height of 1.6mm and a longitudinal spacing and thickness of 0.5mm. For steam, the best-performing tube had circumferential pin thickness and spacing of 0.5 and 1.0mm, respectively, and longitudinal thickness of 0.5mm and spacing of 1.1mm. Tubes with larger fin heights produced higher heat transfer when all other geometric variables remained the same. For R-113, the best-performing tube gave a vapour-side enhancement of 9.9 compared to the plain tube which was about 40% higher than the equivalent integral-fin tube with the same fin height, longitudinal thickness and spacing. For steam, the best-performing tube gave a heat-transfer enhancement of 2.9 compared to the plain tube which was about 25% higher than the equivalent integral-fin tube. For R-113, a near-linear increase in heat-transfer enhancement with active-area enhancement was reported. The heat-transfer enhancement was approximately twice the active-area enhancement. For steam, heat-transfer enhancement was virtually independent of active-area enhancement. The author also reported that static condensate flooding on pin-fin tubes was significantly less than the equivalent integral-fin tubes.

Baiser and Briggs [42] reported experimental data for the condensation of steam at atmospheric pressure and low velocity on five three-dimensional copper pin-fin tubes. These were the same tubes used in the investigations of Briggs [18]. All of the tubes had a pin-fin root diameter of 12.7 mm. Only circumferential thickness and spacing were varied. Vapour-side, heat-transfer coefficients were found by subtracting the coolant and wall resistances from the measured overall thermal resistance. All pin-fin tubes gave higher vapour-side, heat-transfer coefficients compared to the equivalent integral-fin tube. The best heat-transfer enhancement was found to be 4.1 which was thought to be on par with the best-reported heat-transfer enhancement on an optimum integral-fin tube by Wanniarachchi et al. [28]. It was noted that despite less active area of the pin-fin tubes compared to the equivalent integral-fin tube, pin-fin tubes outperformed the integral-fin tube. It was suggested due to the fact that in the case of pin-fin tubes, many small effective surfaces replaced few large surfaces of integral-fin tubes and these smaller surfaces are far more effective for heat transfer since in gravity-drained flows, they result in shorter thinner boundary layers, while for surface-tension-driven flows, these small surfaces produce many more sharp changes in surface curvature, which result in surface-tension-induced pressure gradients which thin the condensate film. An optimum circumferential spacing of 1mm was also identified which maximized the heat-transfer rate.

Ali and Briggs [43–46] have reported a comprehensive data for the condensation of R-113 and ethylene glycol on various pin-fin tubes. Their work has shown superior heat-transfer performance of pin-fin tubes (up to 25%) over the equivalent integral-fin tubes (i.e. with the same fin height, root diameter and longitudinal pin thickness and spacing).

Another useful method to enhance heat transfer on horizontal tubes is by wrapping the wire on the smooth tube; recently, studies are reported by Ali and Qasim [47, 48].

### 3.3. Theoretical studies into condensation heat transfer on enhanced tubes

#### 3.3.1. Tubes with two-dimensional fins

Beatty and Katz [49] were the first to propose a model for condensation heat transfer on integral-fin tubes. The model assumed the following points:

1. Gravity drains the condensate from the vertical fins and from the tube in the inter-fin spacing.
2. Surface-tension effects were entirely ignored, that is, the model did not account for capillary retention on the lower part of the tube or enhanced drainage due to surface tension on the upper part of the tube.
3. The model ignored condensation on the fin tips.

Condensation on the vertical fin flanks was modelled by applying the Nusselt [3] equation for vertical plates and condensation in the inter-fin spacing was modelled by applying the Nusselt [3] equation for horizontal tubes. The mean vapour-side, heat-transfer coefficient for the integral-fin tube was calculated as the area-weighted average of the heat-transfer coefficient on finned surfaces and on base tube between inter-fin spacing. The following expression was suggested for the vapour-side, heat-transfer coefficient:

$$\alpha = c \left[ \frac{k^3 \rho^2 g h_f g}{\mu \Delta T} \right]^{1/4} \left[ \frac{A_r}{A_d} d^{-1/4} + 1.3 \frac{A_f}{A_d} L_f^{-1/4} \right] \quad (17)$$

where  $c$  is an empirical constant and when was taken as 0.689 by Beatty and Katz, their experimental data for six low-surface-tension fluids (methyl chloride, SO<sub>2</sub>, R-22, n-pentane, propane and n-butane) condensing on several integral-fin tubes (with fin densities from 433 to 633 fpm) were predicted within  $\pm 11\%$ .  $L_f$  is the effective fin height (average vertical fin height over the diameter  $d_o$ ), and Beatty and Katz took it as

$$L_f = \frac{\pi}{4} \left[ \frac{d_o^2 - d^2}{d_o} \right] \quad (18)$$

Rose [16] pointed out that if the condensate drained from the fin flanks to the inter-fin space and proceeded to drain around the inter-fin tube surface to the bottom of the tube, then a more appropriate value of the effective fin height would be half of the Beatty and Katz [49] value giving

$$L_f = \frac{\pi}{8} \left[ \frac{d_o^2 - d^2}{d_o} \right] \quad (19)$$

Briggs and Rose [50] compared the Beatty and Katz [49] model to the results of many of the experimental investigations on integral-fin tubes discussed above. The model showed acceptable agreement for relatively low surface-tension fluids but over-predicted the data for high

surface-tension fluids such as steam and ethylene glycol. The authors explained that this was due to the neglect of surface-tension effects in the model.

Gregorig [51] discussed the effect of surface tension and pointed out its vital role in enhancing condensation heat transfer. His work addressed a vertical fluted surface; a schematic is shown in **Figure 6**. The author reported that surface-tension forces are the dominating factor in determining the heat transfer for fins with a height less than 1.5mm, as surface-tension induced pressure gradients due to the variation in the curvature of the vapour-liquid interface of the condensate on the fin. This induced pressure gradient would drain the condensate in the horizontal direction, over the arc length  $S_m$  (see **Figure 6**). The gravity then drains the accumulated condensate from the channels between the flutes. The pressure gradient in the horizontal direction is given by

$$\frac{dP}{dS} = \sigma \frac{d}{dS} \left( \frac{1}{r} \right) \quad (20)$$

where  $S$  is the distance along the vapour-liquid interface from the tip of the fin and  $r$  is the radius of curvature of the liquid-vapour interface. Gregorig [51] also gave a relation that described the shape of a convex profile which provides a constant condensate film thickness over the arc length  $S_m$ ,

$$\frac{1}{r} = \frac{1.5\beta_m}{S_m} \left[ 1 - \left( \frac{S}{S_m} \right)^2 \right] \quad (21)$$

Adamek [52] defined a family of convex shapes that use surface tension to drain the film. His fin curvature was defined as

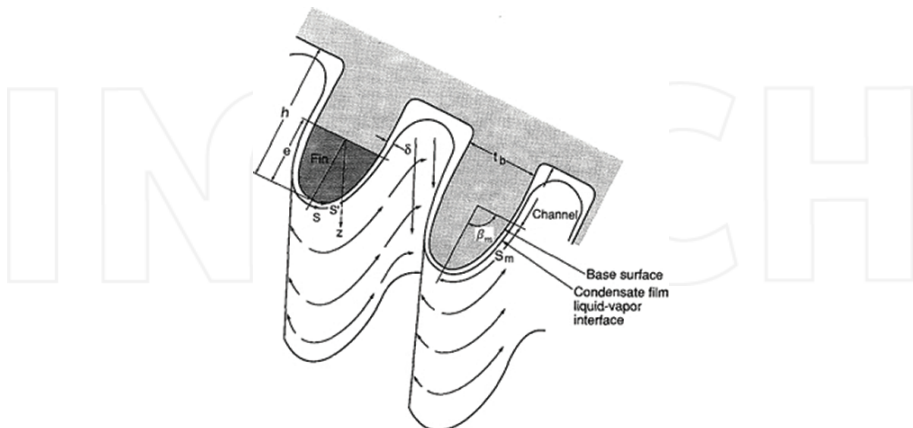


**Figure 6.** Fin parameters of vertical-fluted tube (after Gregorig [51]).

$$\frac{1}{r} = \frac{\beta_m}{S_m} \left( \frac{\zeta + 1}{\zeta} \right) \left[ 1 - \left( \frac{S}{S_m} \right)^\zeta \right] \text{ for } -1 < \zeta < \infty \quad (22)$$

where each value of  $\zeta$  gives a different shape of fin profile and a different aspect ratio  $e/t_b$ . The Adamek [52] profile for a value of  $\zeta = 2$  is identical to the Gregorig [51] profile.

Kedzierski and Webb [53] validated the Gregorig [51] and Adamek [52] theoretical findings. Using an electrostatic discharge-machining method with a numerical-controlled machine head, they produced fin profiles for  $\zeta = 2$  and -0.5. R-11 was used as condensing fluid and experimental data agreed with the predictions to within 5%.

Rudy and Webb [54] presented a model to predict condensation heat-transfer coefficient including the surface-tension effects on fin flanks. Heat transfer through the part of the tube below the flooding angle was not considered. They totally ignored body-forces (gravity) effects on the fin flanks and assumed a constant pressure gradient due to surface tension draining the condensate from the fin flanks into the inter-fin spacing. They took the radius of the curvature of the condensate surface at the fin tip and fin root as half the fin-tip thickness and fin-root spacing, respectively. The result was the following expression for the pressure gradient on the fin flanks:

$$\frac{dP}{dx} = \frac{2\sigma}{h} \left( \frac{1}{s} + \frac{1}{t} \right) \quad (23)$$

Using the above expression to replace the body-force term in the Nusselt expression for the fin flanks, the following result was proposed for vapour-side, heat-transfer coefficient:

$$\alpha = 0.728 \frac{\phi_f}{\pi} \left( \frac{k^3 \rho h_{fg}}{\mu \Delta T} \right)^{1/4} \left[ \frac{A_r}{A_d} \left( \frac{\rho g}{d} \right)^{1/4} + 1.3 \frac{A_f}{A_d} \left\{ \frac{2\sigma}{h^2} \left( \frac{1}{s} + \frac{1}{t} \right) \right\}^{1/4} \right] \quad (24)$$

Honda and Nozu [55] provided a prediction method for heat transfer on horizontal trapezoidal integral-fin tubes. It was pointed out by the authors that an important factor, which had been ignored in earlier theoretical models, is the non-uniformity of wall temperature, due to the large difference in heat-transfer coefficients between the unflooded and flooded regions. Their model incorporated surface tension, gravity and variable wall-temperature effects. The final expression for average heat-transfer coefficient is based on two regions: unflooded and flooded. A numerical analysis has been given just for thin film with the help of the following assumptions:

1. The wall temperature is uniform along the fin.
2. The condensate flow is laminar.
3. The condensate film thickness  $\delta$  is so small that the inertia term in the momentum equation and the convection term in the energy equation can be neglected.
4. Circumferential flow on the flanks can be neglected in comparison with radial flow.

5. Fin height is substantially smaller than the tube outer radius.

The following expression was developed for the condensate film thickness along the fin:

$$\frac{\rho}{3\mu} \frac{d}{dx} \left\{ \left( \rho g f_x - \sigma \frac{d}{dx} \left( \frac{1}{r} \right) \right) \delta^3 \right\} = \frac{k \Delta T}{\delta h_{fg}} \quad (25)$$

$f_x$  is the normalized component of gravity and  $r$  is the radius of curvature of condensate. It should be noted that the analysis is just given for the so-called thin-film regions. For unflooded region, this includes the fin tip, fin corner and fin flank (but not the inter-fin base), whereas for the flooded region it includes only the fin tip and fin corner.

Finally, the following expression was developed for the average Nusselt number for horizontal integral-fin tubes:

$$\frac{\text{Nu}_d = \text{Nu}_{du} \eta_u (1 - \tilde{T}_{wu}) \frac{\phi_f}{\pi} + \text{Nu}_{df} \eta_f (1 - \tilde{T}_{wf}) \left(1 - \frac{\phi_f}{\pi}\right)}{(1 - \tilde{T}_{wu}) \frac{\phi_f}{\pi} + (1 - \tilde{T}_{wf}) \left(1 - \frac{\phi_f}{\pi}\right)} \quad (26)$$

$\tilde{T}_{wu}$  and  $\tilde{T}_{wf}$  are the dimensionless average wall temperatures at the fin roots in the unflooded and flooded regions, respectively, and can be determined by solving the problem for circumferential wall conduction by assuming constant heat-transfer coefficients for the inner surface and for unflooded and flooded regions on the outer surface and neglecting the interaction with radial conduction.  $\eta_u$  and  $\eta_f$  are the fin efficiencies in the unflooded and flooded regions, respectively.  $\text{Nu}_{du}$  and  $\text{Nu}_{df}$  are Nusselt numbers for unflooded and flooded regions, respectively.

Honda and Nozu [55] compared their theoretical model with their own experimental data for the condensation of R-113 and methanol on three integral-fin tubes (see Honda et al. [12]) and found agreement within  $\pm 10\%$ . The same experimental data gave agreement with Beatty and Katz [49] model within  $\pm 20\%$ . They also compared their theoretical model with the experimental results of previous investigators including for 11 fluids and 22 tubes and found an agreement within  $\pm 20\%$ . Briggs and Rose [50] compared the Honda and Nozu [55] model with a range of experimental data of previous investigators and reported that most of the data agreed with the model to within 25%.

Rose [16] pointed out that in most of the proposed heat-transfer models, either gravity was completely neglected when surface-tension-driven drainage was considered on the fin flanks or only the radial component was included. He also suggested the need for a simple heat-transfer model, in the form of an algebraic expression akin of Beatty and Katz [49], but including surface-tension effects. Applying dimensional analysis, the following expression for the mean condensate film thickness was proposed that accounts for both gravity and surface-tension effects:

$$\delta = \left[ \frac{\mu \left( \frac{q}{h_f g \rho} \right)}{\frac{A(\rho - \rho_o)g}{x_g} + \frac{B\sigma}{x_o^3}} \right]^{1/3} \quad (27)$$

$A$  and  $B$  are constants and found separately for the fin tips, fin flanks and inter-fin space.  $x_g$  and  $x_\sigma$  are characteristic lengths for gravity and surface-tension-driven flows, respectively. These characteristic lengths are different for gravity and surface-tension-driven flows. Also, the mean heat flux,  $q$ , through the condensate assuming radial conduction is given as

$$q = \frac{k\Delta T}{\delta} \quad (28)$$

For the fin tip, where there is no retained condensate, the author took the parameters involved in Eq. (27) as  $A = 0.728^4$ ,  $x_g = d_o$ ,  $x_\sigma = t$  and  $B = B_t$  (to be found empirically).

For the unflooded part of the fin flanks, the author took the parameters in Eq. (27) as  $A = 0.943^4$ ,  $x_g = h_v$ ,  $x_\sigma = h$ ,  $B = B_f$  (to be found empirically).  $h_v$  is the mean vertical fin height and was approximated as

$$h_v = \frac{h\emptyset_f}{\sin \emptyset_f} \quad \text{for } \emptyset_f \leq \frac{\pi}{2} \quad (29)$$

$$h_v = \frac{h\emptyset_f}{2 - \sin \emptyset_f} \quad \text{for } \emptyset_f > \frac{\pi}{2} \quad (30)$$

where  $\emptyset_f$  is the flooding angle measured from the top of the tube.

Finally, for the unflooded part of the tube inter-fin space, the author took the parameters in Eq. (27) as  $A = \{\xi(\emptyset)\}^3$ ,  $x_g = d$ ,  $x_\sigma = s$ ,  $B = B_s$  (to be found empirically). The function  $\xi(\emptyset)$  was approximated as

$$\xi(\emptyset) = 0.874 + 0.199110^{-2}\emptyset - 0.264210^{-1}\emptyset^2 + 0.553010^{-2}\emptyset^3 - 0.136310^{-2}\emptyset^4 \quad (31)$$

From Eqs. (27) and (28) with the appropriate values of  $A$ ,  $B$ ,  $x_g$ , and  $x_\sigma$  and neglecting temperature drop in the fin, the mean surface heat flux for the fin tip, fin flank and inter-fin space is given as

$$q_{tip} = \left\{ \frac{\rho h_{fg} k^3 \Delta T^3}{\mu} \left( \frac{0.728^4 (\rho - \rho_v) g}{d_o} + \frac{B_t \sigma}{t^3} \right) \right\}^{1/4} \quad (32)$$

$$q_{flank} = \left\{ \frac{\rho h_{fg} k^3 \Delta T^3}{\mu} \left( \frac{0.943^4 (\rho - \rho_v) g}{h_v} + \frac{B_f \sigma}{h^3} \right) \right\}^{1/4} \quad (33)$$

$$q_{int} = \left\{ \frac{\rho h_{fg} k^3 \Delta T^3}{\mu} \left( \frac{\{\xi(\emptyset)\}^3 (\rho - \rho_v) g}{d} + \frac{B_s \sigma}{s^3} \right) \right\}^{1/4} \quad (34)$$

From Nusselt [3], the expression for the heat flux for a plain tube is

$$q_{\text{plain}} = 0.728 \left\{ \frac{\rho h f_g k^3 \Delta T^3}{\mu} \left( \frac{(\rho - \rho_v) g}{d} \right) \right\}^{1/4} \quad (35)$$

Further, assuming no heat transfer to the flooded and blanked part of fin flanks and inter-fin space, an enhancement ratio for a pitch length of trapezoidal integral-fin tube over the plain tube at the same temperature difference was obtained as

$$\varepsilon_{\Delta T} = \frac{q_{\text{tip}} \pi d_o t + \frac{\emptyset_f}{\pi} \left\{ \frac{q_{\text{flank}} \pi (d_o^2 - d^2) (1-f_f)}{2 \cos \theta} + q_{\text{int}} \pi ds (1-f_s) \right\}}{q_{\text{plain}} \pi d (s+t)} \quad (36)$$

Finally, by substituting Eqs. (32)–(35) for the mean heat flux for fin tip, fin flanks and inter-fin space into Eq. (36), the following final expression is obtained:

$$\begin{aligned} \varepsilon_{\Delta T} = & \frac{d_o t}{d(b+t)} \left( \frac{d}{d_o} + \frac{B_t \sigma d}{0.728^4 (\rho - \rho_v) g t^3} \right)^{1/4} \\ & + \left( \frac{\emptyset_f}{\pi} \right) \left\{ \frac{(1-f_f)(d_o^2 - d^2)}{2d(b+t) \cos \theta} \right\} \left\{ \left( \frac{0.943}{0.728} \right)^4 \left( \frac{d}{h_v} \right) + \frac{B_f \sigma d}{0.728^4 (\rho - \rho_v) g h_v^3} \right\}^{1/4} \\ & + \left( \frac{\emptyset_f}{\pi} \right) \left\{ \frac{(1-f_s)s B_l}{b+t} \right\} \left\{ \frac{\{\xi(\emptyset)\}^3}{0.728^4} + \frac{B_s \sigma d}{0.728^4 (\rho - \rho_v) g s^3} \right\} \end{aligned} \quad (37)$$

In the above expression, to account for the fact that condensate drainage from the fin flanks would affect both gravity and surface-tension contributions to the heat transfer at the inter-fin tube space, a lead constant,  $B_l$ , was introduced in the last term. Moreover, the constants  $B_t$ ,  $B_f$  and  $B_s$  did not differ greatly when found separately, which led to the decision to set these constants equal. Using  $B_t = B_f = B_s = 0.143$  and  $B_l = 2.96$ , the model predicted the dependence of enhancement ratio on fin spacing, fin thickness and fin height excellently. The author pointed out that as the model neglected conduction in the fin, the validity of the model was expected to decrease with decreasing thermal conductivity of the tube material and also with increasing slenderness ratio ( $h/t$ ) of the fin. Briggs and Rose [50] compared the model with a large range of experimental data reported by different investigators. The model predicted most of the data for copper tubes in a range of 20%, whereas it poorly performed for steam condensing on tubes made of bronze with lower thermal conductivity where heat-transfer enhancement was overestimated.

Briggs and Rose [1] incorporated ‘fin efficiency’ effects into the model of Rose [16] in an approximate way. This was done by dividing the tube into flooded and unflooded parts. For the flooded part, the fin flanks were assumed adiabatic to find the heat flux through the fin tip,  $q_{\text{tip,flood}}$ . For the unflooded part, the heat flux for inter-fin space,  $q_{\text{int}}$ , was found using Eq. (34). For the fin flanks and the fin tip in the unflooded part to account for the temperature variations, ‘slender fin’ approximation for the conduction problem was used as follows:

$$\frac{\Delta T(x)}{\Delta T} = \frac{\cosh[m(h-x)] + (\alpha_{tip}/mk_w)\sinh[m(h-x)]}{\cosh(mh) + (\alpha_{tip}/mk_w)\sinh(mh)} \quad (38)$$

where

$$m = \sqrt{\left(\frac{2\alpha_{flank}}{k_w t}\right)} \quad (39)$$

With the help of the above equations, appropriate expressions including temperature variations for flank heat flux,  $q_{flank}$ , and tip heat flux,  $q_{tip}$ , was found for the unflooded area.

Finally, the following expression was proposed to calculate vapour-side, heat-transfer enhancement ratio:

$$\varepsilon_{\Delta T} = \frac{(\pi - \mathcal{O}_f)d_o t q_{tip,flood} + \mathcal{O}_f \left\{ d_o t q_{tip} + (1-f_f) \frac{(d_o^2 - d^2)}{2} q_{flank} \right\} + \mathcal{O}_f (1-f_s) ds q_{int}}{q_{plain} \pi d(s+t)} \quad (40)$$

In the numerator of Eq. (40), the first term shows heat-transfer rate through the flooded part of the tube, the second term shows heat-transfer rate through the unflooded part of the fin and the third term shows heat-transfer rate through the unflooded part of fin spacing. Briggs and Rose [50] compared the experimental data from different investigations to the predictions of the Briggs and Rose [1] model. The inclusion of conduction in the fins on the basis of 'slender fin theory' improved the agreement of experimental data for low thermal conductivity tubes (i.e. bronze tubes condensing steam) with the model.

### 3.3.2. Tubes with three-dimensional fins

Kumar et al. [40] pointed out that almost all the reported heat-transfer models refer to condensation on integral-fin tubes and there was no analytical model for condensation on pin-fin or spine integral-fin tubes. They proposed a generalized empirical model to predict the vapour-side, heat-transfer coefficient for integral-fin as well as pin-fin tubes. They assumed that the heat-transfer coefficient was a function of fluid properties, tube geometry and condensate mass flow rate. This resulted in an expression for the vapour-side, heat-transfer coefficient as follows:

$$\alpha = 0.024(Re)^{-0.333}[We]^{0.3}(Y)^{1.4} \left( \frac{k^3 \rho^2 g}{\mu^2} \right)^{0.333} \quad (41)$$

where all the constants in Eq. (41) were found empirically using least-square method,  $Re$  is the condensate film Reynolds number given by

$$Re = \frac{4\dot{m}}{\mu p} \quad (42)$$

$We$  is the Weber number, the ratio of surface tension and inertia forces in the condensate, and for pin-fin tubes was estimated as a Pythagorean sum of the Weber numbers for the two perpendicular faces of the pins as follows:

$$We = \sqrt{We_l^2 + We_c^2} \quad (43)$$

where  $We_l$  and  $We_c$  are the Webber numbers for the longitudinal and circumferential faces of the pin and are calculated from

$$We_l = \frac{4\sigma(\frac{1}{t_c} + \frac{1}{s_c})}{h\rho g} \quad (44a)$$

$$We_c = \frac{4\sigma(\frac{1}{t_c} + \frac{1}{s_c})}{h\rho g} \quad (44b)$$

Note that for integral-fin tubes, only longitudinal Weber number is used in Eq. (41).

$Y$  is a function of the tube geometry and is given by

$$Y = \frac{4A_o}{dp} = \frac{4\pi}{dp} \left[ \frac{d_o^2 - d^2}{2} + d_o t + d(p - t_b) \right] \quad (45)$$

Kumar et al. [40] compared their own experimental data-condensing steam on two tubes (one integral fin and one pin fin) and R-134a on five tubes (four integral fins and one pin fin) with the model and reported an agreement within 15% for most of the experimental data. Cavallini et al. [56] compared the model to the experimental data for the condensation of steam and refrigerants on integral-fin tubes reported by previous researchers and concluded that the model was not appropriate for tubes with heights of more than 1.1 mm and with fin pitches of more than 1.0 mm or less than 0.5mm for refrigerants and less than 2.0 mm for steam. Namisivayam [57] also compared the model to the experimental data of steam and R-113 on integral-fin tubes and agreed with the conclusions of Cavallini et al. [56].

Belghazi et al. [58] presented a model for a specially designed three-dimensional Gewa C+ tube containing notches around the fin. The tube circumference was divided into flooded and unflooded regions. The authors further divided fin pitch into four regions. It was assumed that for certain regions (i.e. the regions between notches and above notches) surface tension will be the draining force and for other regions (i.e. the region below notches and inter-fin tube space) gravity will be the draining force. Nusselt [3] theory was applied to find the heat-transfer coefficients for the gravity-based drainage regions. By replacing ( $\rho g$ ) in the Nusselt theory with the following expression, surface-tension effects were included in their model:

$$\frac{dF_\sigma}{dV} \approx \frac{\sigma}{h} \left( \frac{1}{r_b} - \frac{1}{r_t} \right) \quad (46)$$

where  $\frac{dF_\sigma}{dV}$  is the volume force,  $r_b$  and  $r_t$  are the radii of curvature of the condensate film liquid-vapour interface at the fin bottom and fin tip, respectively.

The authors compared their model with their own experimental data, for R-134a condensing on a Gewa C+ tube. The model predicted most of the experimental data to within –10%. This

model uses a linear pressure variation technique to account for surface-tension effects and totally ignores gravity effects on the fin notches and above, but still shows a good agreement with experimental data. This might be due to overestimation of surface-tension effects compensating for the absence of gravity.

Ali and Briggs [2] developed a simple semi-empirical correlation accounting for the combined effect of gravity and surface tension for condensation on horizontal pin-fin tubes. The model divided the heat-transfer surface into five regions, that is, two types of pin flank, two types of pin root and the pin tip (**Figure 7**). The following equation was proposed to calculate heat-transfer enhancement:

$$\begin{aligned} \varepsilon_{\Delta T} = & \frac{2t_c t}{0.728\pi d(s+t)} \sum_{i=1}^{n/2} \left[ 0.943^4 \sin \phi \frac{d}{t_c} + B_{tip} \frac{d}{\left(\frac{t_c t}{2(t_c+t)}\right)^3 \tilde{\rho} g} \sigma \right]^{1/4} \\ & + \frac{4ht}{0.728\pi d(s+t)} \sum_{i=1}^{j/2} \left[ 0.943^4 |\cos \phi| \frac{d}{h} + B_{flank1} \frac{d}{\left(\frac{ht}{2(h+t)}\right)^3 \tilde{\rho} g} \sigma \right]^{1/4} \\ & + \frac{4ht_c}{0.728\pi d(s+t)} \sum_{i=1}^{j/2} \left[ 0.943^4 \frac{d}{\frac{ht_c}{\sqrt{h^2+t_c^2 \sin(\phi+\beta)}}} + B_{flank2} \frac{d}{\left(\frac{ht_c}{2(t_c+h)}\right)^3 \tilde{\rho} g} \sigma \right]^{1/4} \\ & + \frac{\phi_f s}{0.728\pi(s+t)} \left[ \{\xi(\phi_f)\}^3 + B_{root1} \frac{d}{\left(\frac{\phi_f ds}{2t_c j}\right)^3 \tilde{\rho} g} \sigma \right]^{1/4} \\ & + \frac{2s_c t}{0.728\pi(s+t)} \sum_{i=1}^{j/2} \left[ 0.943^4 \sin \phi \frac{d}{s_c} + B_{root2} \frac{d}{\left(\frac{s_c}{2}\right)^3 \tilde{\rho} g} \sigma \right]^{1/4} \end{aligned} \quad (47)$$

In Eq. (47),  $\phi$ ,  $\beta$  and  $j$  can be calculated using Eqs. (48)–(50). Only two thermophysical properties are involved in the expression of enhancement ratio, that is, surface tension,  $\sigma$ , and condensate density,  $\rho$ .

$$\phi = \frac{i}{n/2} \pi \quad (48)$$

$$\beta = \tan^{-1}(t_c/h) \quad (49)$$

$$j = n \frac{\phi_f}{\pi} \quad (50)$$

The model gave good overall agreement to within  $\pm 20\%$  with the experimental data, as well as correctly predicted the dependence of heat-transfer enhancement on the various geometric parameters and fluid types.

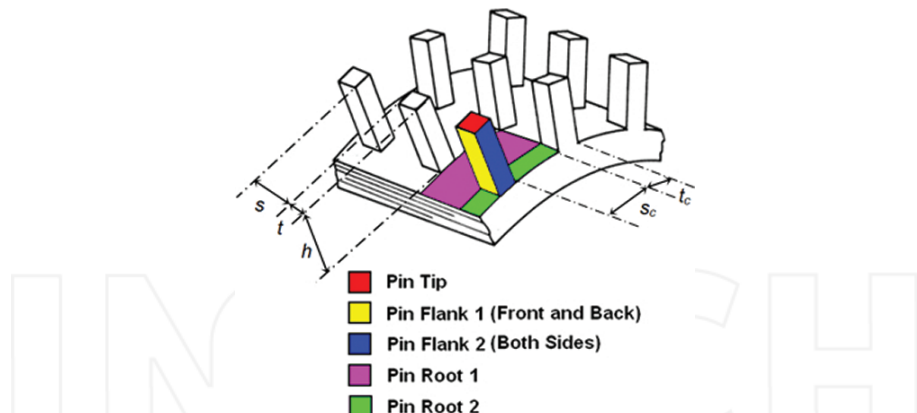


Figure 7. Schematic representation of pin-fin tube identifying five regions for heat transfer (after Ali and Briggs [2]).

#### 4. Conclusions

Extensive experimental work has been performed on integral-fin tubes and has shown that geometry is not the only point of interest for the enhancement of heat transfer. Researchers have reported the optimum fin dimensions for a range of condensing fluids [24–26, 28, 30]. The work of Honda et al. [12] successfully predicts the condensate retention on integral-fin tubes. Reliable heat-transfer models (e.g. [1, 55]) accounting for the combined effects of surface tension and gravity on heat transfer have been developed and are readily available for design engineers.

A reasonable amount of experimental work is reported on condensation heat transfer on enhanced pin-fin tubes. Work of previous researchers has shown the superior performance of such tubes over equivalent integral-fin tubes. The extent of condensate retention and formation of many sharp surfaces enhancing surface-tension effects on pin-fin tubes are identified to be the important parameters contributing towards the heat-transfer enhancement. The model presented by Ali and Briggs [2] is available to predict heat transfer on the pin-fin tubes reasonably by accounting the effect of both gravity and surface-tension condensate drainage.

#### Nomenclature

$A$	constant in Eq. (27)
$A_d$	outside surface area of a smooth tube with outside diameter, $d$
$A_f$	surface area of fin flank
$A_r$	surface area of inter-fin spacing

$B$	constant in Eq. (27)
$B_f$	empirical constant in Eq. (33)
$B_{\text{flank}1}$	empirical constant for pin flank 1
$B_{\text{flank}2}$	empirical constant for pin flank 2
$B_l$	empirical lead constant in Eq. (37)
$B_{\text{root}1}$	empirical constant for root 1
$B_{\text{root}2}$	empirical constant for root 2
$B_s$	empirical constant in Eq. (34)
$B_t$	empirical constant in Eq. (32)
$B_{\text{tip}}$	empirical constant for pin tip
$b$	fin spacing at fin tip or longitudinal pin spacing at pin tip
$c$	constant in Eq. (17)
$d$	outside diameter of plain tube or fin or pin-root diameter of finned or pinned tube
$d_o$	fin or pin-tip diameter of fin or pin tube
$e$	fin height of convex profile
$F_\sigma$	surface-tension force of condensate
$f_f$	blanked proportion of the fin flank for unflooded part of the fin tube
$f_s$	blanked proportion of the inter-fin space for unflooded part of the fin tube
$f_x$	normalized component of gravity (i.e. in horizontal plane)
$g$	specific force of gravity
$j$	number of pins in unflooded region
$h$	fin or pin height
$h_{fg}$	specific enthalpy of vapourization
$h_v$	mean vertical fin or pin height
$k$	thermal conductivity of condensate
$k_w$	thermal conductivity of tube wall
$L$	length of flat plate
$L_f$	mean vertical fin height over diameter $d_o$ defined by Beatty and Katz [49]
$m$	$\sqrt{(2\alpha_{\text{flank}}/k_w t)}$

$\dot{m}$	mass flow rate of condensate
$Nu_d$	average Nusselt number by Honda and Nozu [55] model, defined by Eq. (26)
$Nu_{df}$	Nusselt number for flooded region, Honda and Nozu [55]
$Nu_{du}$	Nusselt number for unflooded region, Honda and Nozu [55]
$Nu_P$	vapour-side Nusselt number for a vertical plate
$Nu_T$	vapour-side Nusselt number for a horizontal tube
$n$	total number of pins per circumference
$p$	fin pitch
$Q$	total heat-transfer rate through the test tube
$q$	heat flux on outside of the test tube
$q_{\text{flank}}$	heat flux to fin flank in unflooded part of the tube
$q_{\text{int}}$	heat flux to inter-fin spacing in unflooded part of the tube
$q_{\text{plain}}$	heat flux through plain or smooth tube
$q_{\text{tip}}$	heat flux to fin tip
$q_{\text{tip, flood}}$	heat flux to fin tip in flooded part of the tube
$Re$	condensate Reynolds number
$R_o$	fin or pin-tip radius
$R_r$	fin or pin-root radius
$r$	radius of curvature of the vapour-liquid interface
$r_b$	radius of curvature of the vapour-liquid interface at fin bottom
$r_t$	radius of curvature of the vapour-liquid interface at fin tip
$S$	distance along the vapour-liquid interface measured from the fin tip
$S_m$	total fin arc length
$s$	fin spacing at fin root or longitudinal pin spacing at pin root
$s_c$	circumferential pin spacing
$\tilde{T}_{wf}$	dimensionless average wall temperatures at fin root in flooded region
$\tilde{T}_{wu}$	dimensionless average wall temperatures at fin root in unflooded region
$t$	fin-tip thickness or longitudinal pin-tip thickness

$t_b$	fin-base thickness or longitudinal pin-base thickness
$t_c$	circumferential pin thickness
$V$	volume of condensate
$We$	Weber number
$We_c$	Weber number for circumferential face of the pin defined by Eq. (44b)
$We_l$	Weber number for longitudinal face of the pin defined by Eq. (44a)
$x$	distance along the vapour-liquid interface measured from the fin tip
$x_g$	characteristic length for gravity-driven flow in Rose [16] model
$x_\sigma$	characteristic length for surface-tension-driven flow in Rose [16] model
$Y$	function of geometric parameters defined by Eq. (45)

#### Greek Letters

$\alpha$	mean vapour-side, heat-transfer coefficient
$\beta$	angle defined by Eq. (49)
$\beta_m$	maximum arc angle
$\Delta T$	temperature difference across the condensate film
$\delta$	condensate film thickness
$\varepsilon_{\Delta T}$	vapour-side, heat-transfer enhancement ratio, heat flux for finned or pinned tube based on fin or pin-root diameter divided by heat flux for smooth tube with the same fin/pin-root diameter, at the same vapour-side, temperature difference
$\zeta$	fin or flute-shape parameter used in Adamek [52] expression
$\eta_f$	fin efficiency for flooded region
$\eta_u$	fin efficiency for unflooded region
$\mu$	dynamic viscosity of condensate
$\xi$	active-area enhancement ratio for fin or pin tube
$\xi(\emptyset)$	function given by Eq. (31)
$\rho$	density of condensate
$\rho_v$	density of vapour
$\tilde{\rho}$	$\rho - \rho_v$
$\sigma$	surface tension

$\theta$	fin or pin-tip half angle
$\emptyset$	angle measured from the top of a fin or a pin tube
$\emptyset_f$	condensate flooding or retention angle measured from the top of a fin or a pin tube

## Author details

Hafiz Muhammad Ali

Address all correspondence to: hafizmali@kfupm.edu.sa; h.m.ali@uettaxila.edu.pk

1 Center of Research Excellence in Renewable Energy (CoRE-RE), King Fahd University of Petroleum & Minerals (KFUPM), Dhahran, Saudi Arabia

2 Department of Mechanical Engineering, University of Engineering and Technology, Taxila, Pakistan

## References

- [1] Briggs, A. and Rose, J. W., (1994), *Effect of Fin Efficiency on a Model for Condensation Heat Transfer on a Horizontal Integral Fin Tube*, Int. J. Heat Mass Transfer, Vol. 37, 457–463.
- [2] Ali, H. M. and Briggs, A. (2015), *A Semi-Empirical Model for Free-Convection Condensation on Horizontal Pin-Fin Tubes*, Int. J. Heat Mass Transfer, Vol. 81, 157–166.
- [3] Nusselt, W., (1916), The Surface Condensation of the Water Vapor, Journal of the Association of German Engineers, Vol. 60, 541–546, 569–575.
- [4] Sparrow, E. M. and Gregg, J. L., (1959), *A Boundary-Layer Treatment of Laminar Film Condensation*, Trans. ASME, Vol. 81, 13–18.
- [5] Koh, J. C. Y., Sparrow, E. M. and Harnett, J. P., (1961), *The Two Phase Boundary Layer in Laminar Film Condensation*, Int. J. Heat Mass Transfer, Vol. 2, 1, 69–82.
- [6] Chen, M. M., (1961), *An Analytical Study of Laminar Film Condensation: Part 1-Flat Plates*, Trans. ASME, Vol. 83, 48–54.
- [7] Chen, M. M., (1961), *An Analytical Study of Laminar Film Condensation: Part 2-Single and Multiple Horizontal Tubes*, Trans. ASME, Vol. 83, 55–60.
- [8] Rose, J. W., (1988), *Fundamentals of Condensation Heat Transfer: Laminar Film Condensation*, JSME Int. J., Vol. 31, 357–375.
- [9] Katz, D. L., Hope, R. E., and Datsko, S. C., (1946), *Liquid Retention on Finned Tubes*, Dept. Eng. Res., Univ. of Michigan, project M592.

- [10] Rudy, T. M., and Webb, R. L., (1985), *An Analytical Model to Predict Condensate Retention on Horizontal Integral Fin Tubes*, Trans. ASME, Vol. 107, 361–368.
- [11] Rudy, T. M., and Webb, R. L., (1981), *Condensate Retention of Horizontal Integral Fin Tubing*, Adv. Enhanced Heat Transfer, ASME HTD, Vol. 18, 35–41.
- [12] Honda, H., Nozu S. and Mitsumori, K., (1983), *Augmentation of Condensation on Finned Tubes by Attaching a Porous Drainage Plate*, Proc. ASME-JSME Therm. Eng. Joint Conf., Vol. 3, 289–295.
- [13] Owen, R. G., Sardesai, R. G., Smith, R. A. and Lee, W. C., (1983), *Gravity Controlled Condensation on Low Integral Fin Tubes*, in *Condenser: Theory and Practice*, 1. Chem. E. Sympos. Serial No. 75, 415–428.
- [14] Yau, K. K., Cooper, J. R., and Rose, J. W., (1986), *Horizontal Plain and Low-Finned Condenser Tubes- Effect of Fin Spacing and Drainage Strips on Heat Transfer and Condensate Retention*, Tran. ASME, Vol. 108, 946–950.
- [15] Masuda, H. and Rose, J.W., (1987), *Static Configuration of Liquid Films on Horizontal Tubes with Low Radial Fins: Implications for Condensation Heat Transfer*, Proc. Roy. Soc., 410, 125–139.
- [16] Rose, J. W., (1994), *An Approximate Equation for the Vapour-side Heat Transfer Coefficient for Condensation on Low Finned Tubes*, Int. J. Heat Mass Transfer, Vol. 37, 865–875.
- [17] Wen, X. L., Briggs, A. and Rose, J. W., (1994), *Enhancement of Condensation Heat Transfer on Integral Fin Tubes Using Radius Fin-Root Fillets*, J. Enhanc. Heat Transfer, Vol. 1, 211–217.
- [18] Briggs, A., (2005), *Liquid Retention on Three-Dimensional Pin-Fin Tubes*, 2nd Int. Exergy, Energy and Environment Symposium, Kos, Paper No. IEEES2-171.
- [19] Ali, H. M. and Briggs, A. (2014), *An investigation of condensate retention on pin-fin tubes*, J. Appl. Therm. Eng., Vol. 63, 503–510.
- [20] Ali, H.M and Abubaker, M. (2014), *Effect of Vapour Velocity on Condensate Retention on Horizontal Pin-Fin Tubes*, Energy Convers. Manage. Vol. 86, 1001–1009.
- [21] Ali, H.M and Ali, A. (2014), *Measurements and Semi-Empirical Correlation for Condensate Retention on Horizontal Integral-Fin Tubes: Effect of Vapour Velocity*, Appl. Therm. Eng., Vol. 71, Issue 1, 24–33.
- [22] Ali, H.M and Abubaker, M. (2015), *Effect of Circumferential Pin Thickness on Condensate Retention as a Function of Vapor Velocity on Horizontal Pin-Fin Tubes*, Appl. Therm. Eng., Vol. 91, 245–251.
- [23] Ali, H. M., Ali, H., Ali, M., Imran, S., Kamran, M. S. and Farukh, F., (2016), *Effect of Condensate Flow Rate on Retention Angle on Horizontal Low-Finned Tubes*, Online, Thermal Science. DOI: 10.2298/TSCI151128211A
- [24] Yau, K. K., Cooper, J. R., and Rose, J. W., (1985), *Effect of Fin Spacing on the Performance of Horizontal Integral-Fin Condenser Tubes*, Tran. ASME, Vol. 107, 377–383.

- [25] Masuda, H. and Rose, J.W., (1985), *An Experimental Study of Condensation of R-113 on Low Integral-Fin Tubes*, Proc. Int. Symp. Heat Transfer., 2, Paper No. 32.
- [26] Masuda, H. and Rose, J.W., (1988), *Condensation of Ethylene Glycol on Horizontal Finned Tubes*, Trans. ASME, Vol. 110, 1019–1022.
- [27] Wanniarachchi, A. S., Marto, P. J. and Rose, J. W., (1985), *Film Condensation of Steam on Horizontal Finned Tubes: Effect of Fin Spacing, Thickness and Height*, Multiphase Flow Heat Transfer, ASME HTD, Vol. 47, 93–99.
- [28] Wanniarachchi, A. S., Marto, P. J. and Rose, J. W., (1986), *Film Condensation of Steam on Horizontal Finned Tubes: Effect of Fin Spacing*, Tran. ASME, Vol. 108, 960–966.
- [29] Marto, P. J., Mitrou, E., Wanniarachchi, A. S., and Rose, J. W., (1986), *Film Condensation of Steam on Horizontal Finned Tubes: Effect of Fin Shape*, Proc. 8th Int. Heat Transfer Conf., Vol. 4, 1695–1700.
- [30] Marto, P. J., Zebrowski, D., Wanniarachchi, A. S. and Rose, J. W., (1990), *An Experimental Study of R-113 Film Condensation on Horizontal Integral Fin Tubes*, Trans. ASME, Vol. 112, 759–767.
- [31] Briggs, A. Wen, X. L. and Rose, J. W., (1992), *Accurate Heat Transfer Measurements for Condensation on Horizontal, Integral-Fin Tubes*, Trans. ASME, Vol. 114, 719–726.
- [32] Briggs, A., Song Huang, X. and Rose, J. W., (1995), *An Experimental Investigation of Condensation on Integral Fin Tubes: Effect of Fin Thickness, Height and Thermal Conductivity*, Proc. ASME Nat. Heat Transfer Conf., HTD, Vol. 308, 21–29.
- [33] Park, K. J. and Jung, D., (2008), *Optimum Fin Density of Low Fin Tubes for the Condensers of Building Chillers with HCFC123*, J. Energy Conserv. Manage., Vol. 49, 2090–2094.
- [34] Sukhatme, S. P., Jagadish, B. S. and Prabhakaran, P., (1990), *Film Condensation of R-11 Vapor on Single Horizontal Enhanced Condenser Tubes*, Trans. ASME, Vol. 112, 229–234.
- [35] Briggs, A., Yang, X. X. and Rose, J. W., (1995), *An Evaluation of Various Enhanced Tubes for Shell-Side Condensation of Refrigerant*, Heat Transfer in Condensation, Proc. Eurotherm. Semin. No. 47, Paris, Elsevier Pub. Co., 62–70.
- [36] Cheng, W. Y., Wang, C. C., Robert Hu, Y. Z. and Huang, L. W., (1996), *Film Condensation of HCFC-22 on Horizontal Enhanced Tubes*, Int. Comm. Heat Mass Transfer, Vol. 23, 79–90.
- [37] Kumar, R., Varma, H. K., Mohanty, B. and Agrawal, K. N., (1998), *Augmentation of Outside Tube Heat Transfer Coefficient during Condensation of Steam over Horizontal Copper Tubes*, Int. Comm. Heat Mass Transfer, Vol. 25, 81–91.
- [38] Jung, D. S., Kim, C. B., Cho, S. and Song, K., (1999), *Condensation Heat Transfer Coefficients of Enhanced Tubes with Alternative Refrigerants for CFC11 and CFC12*, Int. J. Refriger., Vol. 22, 548–557.
- [39] Kumar, R., Varma, H. K., Mohanty, B. and Agrawal, K. N., (2002), *Augmentation of Heat Transfer During Filmwise Condensation of Steam and R-134a over Single Horizontal Finned Tubes*, Int. J. Heat Mass Transfer, Vol. 45, 201–211.

- [40] Kumar, R., Varma, H. K., Mohanty, B. and Agrawal, K. N., (2002), *Prediction of Heat Transfer Coefficient During Condensation of Water and R-134a on Single Horizontal Integral-Fin Tubes*, Int. J. Refriger., Vol. 25, 111–126.
- [41] Briggs, A., (2003) *Enhanced Condensation of R-113 and Steam on Three-Dimensional Pin-Fin Tubes*, J. Exp. Heat Transfer, Vol. 16, 61–79.
- [42] Baiser, M., and Briggs, A., (2009), *Condensation of Steam on Pin-Fin Tubes: Effect of Circumferential Pin Thickness and Spacing*, J. Heat Transfer Eng., Vol. 30, 1017–1023.
- [43] Ali, H. M. and Briggs, A. (2012), *Condensation of R-113 on Pin-Fin Tubes: Effect of Circumferential Pin Thickness and Spacing*, Heat Transfer Eng., Vol. 33, Issue 3, 205–212.
- [44] Ali, H. M. and Briggs, A. (2012), *Condensation of Ethylene Glycol on Pin-Fin Tubes: Effect of Circumferential Pin Thickness and Spacing*, Appl. Therm. Eng., Vol. 49, 9–13.
- [45] Ali, H. M. and Briggs, A. (2012), *Enhanced Condensation of Ethylene Glycol on Pin-Fin Tubes: Effect of Pin Geometry*, ASME J. Heat Transfer, Vol. 134, 011503.
- [46] Ali, H. M. and Briggs, A. (2013), *Condensation Heat Transfer on Pin-Fin Tubes: Effect of Thermal Conductivity and Pin Height*, Appl. Therm. Eng., Vol. 60, 465–471.
- [47] Ali, H. M. and Qasim, M. Z. (2015), *Free Convection Condensation of Steam on Horizontal Wire Wrapped Tubes: Effect of Wire Thermal Conductivity, Pitch and Diameter*, Appl. Therm. Eng., Vol. 90, 207–214.
- [48] Ali, H. M., Qasim, M. Z. and Ali, M. (2016), *Free Convection Condensation Heat Transfer of Steam on Horizontal Square Wire Wrapped Tubes*, Int. J. Heat Mass Transfer, Vol. 98, 350–358.
- [49] Beatty, K. O., and Katz, D. L., (1948), *Condensation of Vapors on Outside of Finned Tubes*, Chem. Eng. Prog., Vol. 44, 55–70.
- [50] Briggs, A. and Rose, J. W., (1999), *An Evaluation of Models for Condensation Heat Transfer on Low-Finned Tubes*, J. Enhanc. Heat Transfer, Vol. 6, 51–60.
- [51] Gregorig, R., (1954), Film Condensation on Fine-Walled Surfaces, taking into account the Surface Tension, Journal of Applied Mathematics and Physics, Vol. 5, 36–49.
- [52] Adamek, T., (1981), Determination of Condensation on Finely Corrugated Surfaces Design of Optimal Wall Profiles, Waerme- and Stoffue-bertragung, Vol. 15, 255–270.
- [53] Kedzierski, M.A. and Webb, R.L., (1987), *Experimental Measurements of Condensation on Vertical Plates with Enhanced Fins*, ASME. Boil. Condens. Heat Transfer Equip., HTD, Vol. 85, 87–95.
- [54] Rudy, T. M., and Webb, R. L., (1983), *Theoretical Model For Condensation on Horizontal Integral-Fin Tubes*, Am. Inst. Chem. Eng. Symp. Ser., Vol. 79, 11–18.
- [55] Honda, H. and Nozu S., (1987), *A Prediction Method for Heat Transfer During Film Condensation on Horizontal Low Integral Fin Tubes*, Trans. ASME, Vol. 109, 218–225.
- [56] Cavallini, A., Cesni, G., Del Col, D., Doretti, L., Longo, G. A., Rossetto, L. and Zilio, C., (2003), *Condensation Inside and Outside Smooth and Enhanced Tubes: A Review of Recent Research*, Int. J. Refriger., Vol. 26, 373–392.

- [57] Namasivayam, S., (2006), *Condensation on Single Horizontal Integral-Fin Tubes: Effect of Vapour Velocity and Fin Geometry*, PhD Thesis, University of London.
- [58] Belghazi, M., Bontemps, A. and Marvillet, C., (2002). *Condensation Heat Transfer on Enhanced Surface Tubes: Experimental Results and Predictive Theory*, Trans. ASME, Vol. 124, 754–761.